

lacking symbionts (14), and more genera of carbonate platform gastropods became extinct than did those from other regions and environments, even within the tropics (15). These data argue for habitat selectivity, but only for carbonate platforms and associated lagoons in the tropics. Certain microplankton groups also suffered greater extinction in the tropics than in polar regions (16), but here too the pattern may reflect disruption of particular habitats rather than a true latitudinal gradient (17).

Taken together, our analyses indicate that the end-Cretaceous mass extinction was a globally uniform event. Although this result does not verify bolide impact or any other proposed cause of the extinction, it does rule out mechanisms having purely regional or latitudinal effects.

REFERENCES AND NOTES

1. D. Jablonski, *Science* 253, 754 (1991).
2. The term is from N. Myers [*The Environmentalist* 10, 243 (1990)].
3. S. M. Stanley, in *Extinctions*, M. H. Nitecki, Ed. (Univ. of Chicago Press, Chicago, 1984), pp. 69–117; *Am. J. Sci.* 288, 334 (1988); D. Jablonski, in *Dynamics of Extinction*, D. K. Elliott, Ed. (Wiley, New York, 1986), pp. 183–229; W. J. Zinsmeister, R. M. Feldmann, M. O. Woodburne, D. H. Elliott, *J. Paleontol.* 63, 731 (1989).
4. A full bibliography of sources is available from the authors.
5. P. D. Ward, *Geol. Soc. Am. Spec. Pap.* 247, 425 (1990); E. G. Kauffman, in *Global Bio-Events*, O. H. Walliser, Ed. (Springer-Verlag, Berlin, 1986), pp. 279–335.
6. J. J. Sepkoski, Jr., *J. Geol. Soc. London* 146, 7 (1989); *Geol. Soc. Am. Spec. Pap.* 247, 33 (1990).
7. D. Jablonski, *Science* 231, 129 (1986); *Philos. Trans. R. Soc. London Ser. B* 325, 357 (1989); S. R. Westrop, *Paleobiology* 15, 46 (1989); D. H. Erwin, *Palaos* 4, 424 (1989).
8. Consider an extreme, hypothetical case of seven genera: one nonsurviving genus confined to each of the six regions in Fig. 1 and one surviving genus that is cosmopolitan, occurring in all regions. Each region shows 50% extinction (one out of two), whereas the global sample shows 86% extinction (six out of seven).
9. V. L. Sharpton et al., *Nature* 359, 819 (1992).
10. E. G. Kauffman and C. C. Johnson, *Palaos* 3, 194 (1988).
11. J.-P. Masse and J. Philip, *Bull. Cent. Rech. Explor.-Prod. Elf-Aquitaine* 10, 437 (1986); C. C. Johnson and E. G. Kauffman, in *Extinction Events in Earth History*, E. G. Kauffman and O. H. Walliser, Eds. (Springer-Verlag, Berlin, 1990), pp. 305–324.
12. K. G. MacLeod and P. D. Ward, *Geol. Soc. Am. Spec. Pap.* 247, 509 (1990).
13. High-latitude extinction intensities might decrease slightly with inclusion of the Ocean Point fauna from North Slope, Alaska, which is mostly undescribed and may be either latest Cretaceous or earliest Tertiary in age [L. Marinovich, Jr., et al., *Geology* 13, 770 (1985); T. R. Waller and L. Marinovich, Jr., *J. Paleontol.* 66, 215 (1992)]. The effect of this fauna on our analyses will depend on its geologic age: if Tertiary, it includes survivors with various biogeographic affinities; if Maastrichtian, it contains several high-latitude precursors of typically Cenozoic taxa.
14. B. R. Rosen and D. Turnsek, *Mem. Assoc. Australas. Paleontol.* 8, 355 (1989).
15. N. F. Sohl, *J. Paleontol.* 61, 1085 (1987).
16. K. Perch-Nielsen et al., *Geol. Soc. Am. Spec. Pap.* 190, 353 (1982); G. Keller, *Geol. Soc. Am. Bull.* 101, 1408 (1989).

17. J. H. Lipps, in *Dynamics of Extinction*, D. K. Elliott, Ed. (Wiley, New York, 1986), pp. 87–104; J. C. Zachos and M. A. Arthur, *Paleoceanography* 1, 5 (1986).
18. With less than 25 rudist genera ($n < 25$), scatter due to sampling error becomes extreme. For example, with $n = 10$, a true extinction of 50%, and random sampling, the 68% confidence limits are 33.9 and 66.1%, and the 95% confidence limits are 18.2 and 81.8%. Given that the total number of samples being considered is relatively small, extinction values based on the smaller samples are virtually meaningless.
19. We calculated standard errors explicitly by summing binomial probabilities using a program given by D. M. Raup, in *Analytical Paleobiology*, N. L. Gilinsky and P. W. Signor, Eds. (Paleontological Society, Knoxville, TN, 1991), pp. 207–216. For the range of sample sizes we used, the results are virtually identical to standard errors estimated from conventional approximation formulas.
20. The surface area contained in a 10° latitude-longitude block naturally decreases with distance

from the equator. Therefore, Fig. 1 should not be used to assess biologic diversity (genera per unit area). However, the latitude effect does not influence the comparisons of extinction intensities (percentages) considered in this report.

21. We thank R. J. Cleevely, A. V. Dhondt, C. Heinberg, C. C. Johnson, E. G. Kauffman, G. L. Kennedy, N. Malchus, M. Machalski, N. J. Morris, L. R. Saul, J. J. Sepkoski, Jr., N. F. Sohl, T. R. Waller, and L. R. Wingard for advice and access to collections or information. We thank D. B. Rowley (Paleogeographic Atlas Project, University of Chicago) for the Maastrichtian latitude-longitude conversions for bivalve sample sites. Special thanks go to A. Koziol, D. McShea, and J. Schneider for undertaking the initial literature search and data compilation that served as the skeleton for development of the full database. Supported by National Aeronautics and Space Administration grants NAGW-1508 and 1527 (D.M.R.) and NSF grants EAR90-05744 and INT86-2045 (D.J.).

7 December 1992; accepted 11 February 1993

Interaction of the San Jacinto and San Andreas Fault Zones, Southern California: Triggered Earthquake Migration and Coupled Recurrence Intervals

Christopher O. Sanders

Two lines of evidence suggest that large earthquakes that occur on either the San Jacinto fault zone (SJFZ) or the San Andreas fault zone (SAFZ) may be triggered by large earthquakes that occur on the other. First, the great 1857 Fort Tejon earthquake in the SAFZ seems to have triggered a progressive sequence of earthquakes in the SJFZ. These earthquakes occurred at times and locations that are consistent with triggering by a strain pulse that propagated southeastward at a rate of 1.7 kilometers per year along the SJFZ after the 1857 earthquake. Second, the similarity in average recurrence intervals in the SJFZ (about 150 years) and in the Mojave segment of the SAFZ (132 years) suggests that large earthquakes in the northern SJFZ may stimulate the relatively frequent major earthquakes on the Mojave segment. Analysis of historic earthquake occurrence in the SJFZ suggests little likelihood of extended quiescence between earthquake sequences.

Historically, large earthquakes have occurred in the SJFZ in 1899, 1918, 1923, 1937, 1954, 1968, 1969, and 1987 (see Table 1 for source parameters and references). These earthquakes were preceded by the moment magnitude (M) 8 Fort Tejon earthquake of 1857 that ruptured ~ 360 km of the SAFZ from near Cholame to Cajon Pass with 3 to 9 m of right slip (1) (Fig. 1). At its southeastern end, the 1857 rupture probably terminated in the Cajon Pass area (1, 2). The SJFZ branches from the SAFZ in the Cajon Pass area (Fig. 1); northwest of the pass the SAFZ accommodates right slip of ~ 3.5 cm year $^{-1}$ (3), whereas southeast of the pass it accommodates ~ 2.5 cm year $^{-1}$ (4, 5), with ~ 1 cm year $^{-1}$ (6–8) accommodated by the SJFZ.

Although attention previously has focused primarily on the SJFZ and SAFZ as separate mechanical entities, structural and

geodetic evidence clearly shows that the fault zones are closely linked. For instance, the 1857 rupture terminated to the southeast near the area where the SJFZ branches from the SAFZ; this coincidence has been appreciated in notions of fault zone segmentation (9–11). In this report, I investigate the triggering of large earthquakes in either fault zone by large earthquakes in the other.

The primary data for this analysis are the recorded dates of occurrence, the epicenters and rupture lengths, the seismic moments, and the down-dip rupture widths of large earthquakes in the SJFZ (Table 1). The dates and times of occurrence and the epicenters of the large earthquakes in the SJFZ were obtained from compilations of historical accounts of major ground shaking (12–14) and from the catalog of instrumentally determined earthquake locations assembled by the California Institute of Technology and the U.S. Geological Survey. In some cases, the epicenters used are from relocation studies (15, 16). The rupture

Department of Geology, Arizona State University, Tempe, AZ 85287-1404.

lengths for the earthquakes were obtained from reports of surface rupture, aftershock locations, and source process time where available. The down-dip widths of the rupture zones were estimated from the hypocentral depths of the main shocks and from

studies of the seismicity and strain in the fault zone (17).

When the large earthquakes in the SJFZ are plotted by origin time and epicenter, a consistent relation emerges (Fig. 2). From the northwest end of the fault zone near the

termination of the 1857 San Andreas rupture to near the southeast end of the fault zone, a line with a slope of 1.7 km year^{-1} passes through or near seven of the nine earthquakes plotted, including all of the largest earthquakes. (The 1923 and 1969 earthquakes, which plot farthest from the line, are reasonably explained as related to local stress concentrations at the ends of the large 1899 to 1918 and 1968 earthquake sequences, respectively.) One explanation for this migration is that the 1857 rupture on the SAFZ initiated a strain pulse at the southeast end of the 1857 rupture that propagated southeastward along the SJFZ and triggered large earthquakes as it passed. Because not all segments of the fault zone ruptured after the passage of this strain pulse, it appears that only those segments already sufficiently close to failure were triggered by the transient strain increase. Segments that did not break may have broken earlier, independently of this strain pulse and before it arrived. Such ruptures may include poorly located earthquakes in 1890 and 1892, which possibly occurred in the central SJFZ (12).

The 1948 Desert Hot Springs earthquake, which occurred on or near the northern end of the Indio segment of the SAFZ (13, 18) (Figs. 1 and 2), also occurred at a time and place that are fairly consistent with triggering by the proposed strain pulse. This correlation suggests that a strain pulse traveled along the southern SAFZ as well but triggered only one earthquake.

Earthquake migration has been observed previously. A famous example is the sequence of earthquakes in the strike-slip North Anatolian fault zone during the years 1939 to 1964 (19–21). The sequence began with a magnitude (M) 7.9 earthquake. The westward migration rate of the next three M 7.0 to 7.4 events, whose rupture zones

Fig. 1. Map of the SJFZ and SAFZ in southern California. L.A., Los Angeles. Modified from (29).

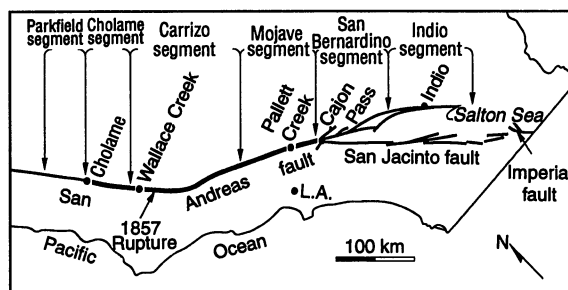


Fig. 2. Plot of the locations of large earthquakes in the SJFZ versus time. The fault segments of the SJFZ are mapped in the upper part of the figure, and the epicenters and probable rupture zones of the large earthquakes are indicated. A line with a slope (strain propagation) of 1.7 km year^{-1} connects the 1857, 1899, 1918, 1937, 1954, 1968, and 1987 earthquakes. The relatively small 1923 and 1969 earthquakes fall off of the line. However, their positions may be related to triggering near the ends of the 1899 to 1918 and 1968 earthquakes, respectively, rather than to triggering by the proposed strain pulse. In addition, the 1948 Desert Hot Springs earthquake near or on the southern SAFZ is plotted with the SJFZ earthquakes to show its general consistency with the triggering hypothesis. The values of average displacement, determined with the use of the measured seismic moments and rupture areas, are indicated in parentheses.

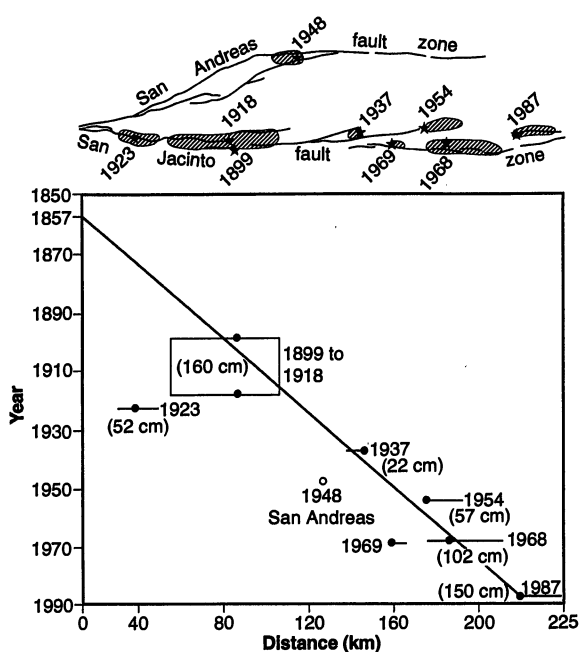


Table 1. Source parameters of the SJFZ and SAFZ earthquakes discussed. Dates are given as year, month, day; locations are latitude, longitude, with degree and minute values given when known; M is

moment magnitude; M is magnitude; M_i is intensity magnitude; M_L is local magnitude; M_0 is the moment in dyne-centimeters $\times 10^{25}$; L is rupture length in kilometers; and Z is hypocentral depth in kilometers.

Date	Location	M	M_0	L	Z	References
1857, 1, 9*	San Andreas	M 8	~ 700	≥ 360	10 to 15	(1, 2)
1858, 12, 6	San Bernardino	M ~ 6				(12)
1890, 2, 9	Central SJFZ	M_i 6.3	~ 15			(12, 32)
1892, 5, 28	Central SJFZ	M_i 6.3				(12)
1899, 7, 22	Cajon Pass	M_i 6.7				(12)
1899, 12, 25*	$\sim 33^\circ 47', 117^\circ 00'$	M_i 6.7	~ 15	25 ± 5		(12, 32)
1918, 4, 21*	$\sim 33^\circ 52', 117^\circ 02'$	M 6.8	14 ± 5	27 ± 5	7 ± 5	(13, 14, 32, 33)
1923, 7, 23*	$\sim 34^\circ 05', 117^\circ 20'$	M 6.3	2.6 ± 0.5	11 to 18	12 ± 2	(13–15, 32, 33)
1937, 3, 25*	$33^\circ 27.9', 116^\circ 24.9'$	M 5.6	0.5 ± 0.2	8 ± 1	3 ± 2	(13, 16, 32, 34, 35)
1948, 12, 4*	$33^\circ 55.2', 116^\circ 28.9'$	M_L 6.5		13	12	(13, 18)
1954, 3, 9*	$33^\circ 17.7', 116^\circ 10.6'$	M 6.3	2.4 ± 0.3	14	9 ± 4	(13, 16, 34–36)
1968, 4, 9*	$33^\circ 11.4', 116^\circ 07.7'$	M 6.7	11 ± 1	36 ± 3	10 ± 1	(32, 37–44)
1969, 4, 28*	$33^\circ 20.6', 116^\circ 20.8'$	M 5.7	0.4 ± 0.1	8	12 ± 2	(34, 44, 45)
1987, 11, 24*	$33^\circ 00.0', 115^\circ 50.9'$	M 6.6	10.5 ± 0.5	27	9 ± 1	(46–49)

*These dates are plotted on Fig. 2. The other entries may have occurred in the SJFZ, but their locations are poorly known.

abuted, was $\sim 150 \text{ km year}^{-1}$. However, the migration rate for the entire sequence of ten M 5.9 to 7.4 events, which contained unruptured gaps between some rupture zones, was $\sim 40 \text{ km year}^{-1}$ (21). Also, eight M 5.9 to 7.3 events migrated eastward from the initial 1939 earthquake at a rate of $< 10 \text{ km year}^{-1}$ (21). Another migration of large crustal earthquakes occurred during the years 1923 to 1970 on the Japanese island of Honshu. After the M 7.9 Kanto earthquake, nine M 6.0 to 7.3 earthquakes occurred in a generally northward progressive manner, with intervening unruptured gaps with an average migration rate of $\sim 10 \text{ km year}^{-1}$ (22). Other examples of earthquake or strain migration in the Japanese, California, and circum-Pacific regions include 3 km year^{-1} for $M \geq 5.0$ events (23), 20 km year^{-1} for $M \geq 6.0$ events (22), 60 km year^{-1} for M 7.5 to 8.3 events (22), 60 km year^{-1} for $M \geq 7.9$ events (24), 150 to 270 km year^{-1} for $M \geq 8.2$ events (22), and 20 km year^{-1} for tilt events (25).

The question is whether these observations indicate the action of a predictable physical mechanism or are the product of random chance. Because most migrations of $M \geq 6$ earthquakes were immediately preceded by great $M \geq 7.9$ earthquakes, the migrations may be a physical result of the considerable strain release from the great earthquake ruptures (22). Models of propagating deformation that results from fault rupture indicate that for propagation speeds on the order of 100 km year^{-1} or more, elastic interactions of adjacent rupture segments in a fault zone will predominate, whereas at lesser speeds the viscoelastic properties of the lower crust and upper mantle play the principal role in the slow propagation of the deformation front (24, 26, 27). This relation implies that the observed 1.7 km year^{-1} migration rate of the historical M 5.9 to 6.8 earthquakes in the SJFZ resulted from slow strain redistribution by viscoelastic processes in the lower crust and upper mantle after the great 1857 SAFZ earthquake.

As of 1987, the strain pulse had traveled to the southern end of the SJFZ; if it continues propagating southward, the next major fault it encounters will be the Imperial fault (Fig. 1). The northern half of this fault ruptured in 1979 and 1940, while the southern half has not ruptured since 1940 (28). Rupture of the southern Imperial fault in 20 to 40 years would be consistent with triggering by the strain pulse.

The earthquake record for the past millennium on the Mojave, Carrizo, and Indio segments of the SAFZ has been revealed by studies at Pallett Creek, Wallace Creek, and Indio, respectively (Fig. 1). At Wallace Creek, the slip rate has been determined as 3.4 cm year^{-1} , the surface slip

during the 1857 earthquake was 9.5 m, the surface slip during the earlier two major earthquakes was 12.3 m and 11.5 m, and the calculated recurrence intervals range from 240 to 450 years (1, 3). At Pallett Creek, the surface slip during the 1857 earthquake was 4 m and the recurrence interval for the past nine major earthquakes averages 132 years (range from 44 to 332 years) (1, 29). At Indio, the recurrence intervals since A.D. 1000 range from 150 to > 300 years, averaging ~ 250 years (30). On the basis of the observation that the Mojave segment (Pallett Creek) experiences major fault rupture about twice as often but with one-half the surface slip as the Carrizo segment (Wallace Creek), Sieh and colleagues (29, 31) proposed that the earthquake cycle on the Mojave segment includes alternating Carrizo plus Mojave and Mojave plus Indio ruptures. That is, they suggested that the Mojave segment ruptures twice as often as either the Carrizo or Indio segments because it is included in the southern end of Carrizo ruptures and in the northern end of Indio ruptures.

I suggest another possibility, namely, that earthquakes in the SJFZ may stimulate the relatively frequent earthquake occurrence in the Mojave segment of the SAFZ. The geometric continuity of the SJFZ and the SAFZ near their intersection suggests that deformation on the northern SJFZ should influence deformation on the Mojave segment of the SAFZ. To investigate this effect, I compared the time scales of the earthquake cycles in the two fault zones. In the SJFZ the characteristic slip in the sections that contained the largest historic earthquakes was $\sim 150 \text{ cm}$ (for the measured moments and rupture lengths and a rupture depth of 10 km) (Fig. 2 and Table 1), and the long-term slip rate in the fault zone has been $\sim 1 \pm 0.2 \text{ cm year}^{-1}$ (6–8), therefore, rupture of these sections should recur about every 150 ± 30 years. If the historic slip is representative of the slip that occurs all along the fault zone in one complete seismic cycle, then all of the segments of the SJFZ should rupture about every 150 years. This period is similar to the mean recurrence interval of 132 years for rupture of the Mojave segment of the SAFZ. If on the average of every 150 years large earthquakes rupture the segments of the SJFZ that abut the Mojave segment of the SAFZ, then the concentrated stress increase could help induce rupture of the Mojave segment on a similar time scale.

The Anatolian earthquake sequences during the past two millennia were interspersed with periods of quiescence of ~ 150 years (19, 20). It appears that the North Anatolian fault zone ruptures during a relatively short time in a sequence of large earthquakes and then becomes quiet for an

extended period. In contrast, the historic record suggests that the pattern on the SJFZ will be different. During the 90-year period of 1899 to 1987, scattered segments that total about one-half of the length of the SJFZ have ruptured; at this rate all segments of the fault zone should rupture in less than 180 years. This period is similar to the ~ 150 -year recurrence time calculated above for rupture of the SJFZ. Thus, at least at the current rate of segment rupture, we should not expect an extended period of quiescence to follow the historic earthquake sequence in the SJFZ.

REFERENCES AND NOTES

1. K. E. Sieh, *Bull. Seismol. Soc. Am.* **68**, 1421 (1978).
2. D. C. Agnew and K. E. Sieh, *ibid.*, p. 1717.
3. K. E. Sieh and R. H. Jahns, *Geol. Soc. Am. Bull.* **95**, 883 (1984).
4. R. J. Weldon II and K. E. Sieh, *ibid.* **96**, 793 (1985).
5. J. W. Harden and J. C. Matti, *ibid.* **101**, 1107 (1989).
6. R. V. Sharp, *ibid.* **78**, 705 (1967).
7. ———, *J. Geophys. Res.* **86**, 1754 (1981).
8. T. Rockwell, C. Loughman, P. Merifield, *ibid.* **95**, 8593 (1990).
9. C. R. Allen, *Stanford Univ. Publ. Geol. Sci.* **11**, 70 (1968).
10. R. Weldon and J. Matti, *Eos* **67**, 905 (1986).
11. C. O. Sanders, *U. S. Geol. Surv. Open-File Rep.* **89-315** (1989), p. 324.
12. T. R. Topozada, C. R. Real, D. L. Parke, *Calif. Div. Mines Geol. Open-File Rep.* **81-11 SAC** (1981).
13. C. F. Richter, *Elementary Seismology* (Freeman, San Francisco, 1958).
14. T. R. Topozada and D. L. Parke, *Calif. Div. Mines Geol. Open-File Rep.* **82-17 SAC** (1982).
15. C. O. Sanders and H. Kanamori, *J. Geophys. Res.* **89**, 5873 (1984).
16. C. Sanders, H. Magistrale, H. Kanamori, *Bull. Seismol. Soc. Am.* **76**, 1187 (1986).
17. C. O. Sanders, *J. Geophys. Res.* **95**, 4751 (1990).
18. C. Nicholson, *Seismol. Res. Lett.* **58**, 14 (1987).
19. N. N. Ambraseys, *Tectonophysics* **9**, 143 (1970).
20. C. R. Allen, *Geol. Soc. Am. Bull.* **86**, 1041 (1975).
21. M. N. Toksoz, A. G. Shakal, A. J. Michael, *Pure Appl. Geophys.* **117**, 1258 (1979).
22. K. Mogi, *Earthquake Prediction* (Academic Press, Tokyo, 1985).
23. M. D. Wood and S. S. Allen, *Nature* **244**, 213 (1973).
24. J. C. Savage, *J. Geophys. Res.* **76**, 1954, (1971).
25. K. Kasahara, *Philos. Trans. R. Soc. London Ser. A* **274**, 287 (1973).
26. M. H. P. Bott and D. S. Dean, *Nature* **243**, 339 (1973).
27. F. K. Lehner, V. C. Li, J. R. Rice, *J. Geophys. Res.* **86**, 6155 (1981).
28. R. V. Sharp, *U.S. Geol. Surv. Prof. Pap.* **1254** (1982), p. 213.
29. K. Sieh, M. Stuijver, D. Brillinger, *J. Geophys. Res.* **94**, 603 (1989).
30. K. Sieh, *Eos* **67**, 1200 (1986).
31. K. E. Sieh, *J. Geophys. Res.* **83**, 3907 (1978).
32. T. C. Hanks, J. A. Hileman, W. Thatcher, *Geol. Soc. Am. Bull.* **86**, 1131 (1975).
33. D. I. Doser, *Bull. Seismol. Soc. Am.* **82**, 1786 (1992).
34. A. L. Bent and D. V. Helmberger, *ibid.* **81**, 2289 (1991).
35. D. I. Doser, *ibid.* **80**, 1099 (1990).
36. W. Thatcher and T. C. Hanks, *J. Geophys. Res.* **78**, 8547 (1973).
37. C. R. Allen and J. M. Nordquist, *U.S. Geol. Surv. Prof. Pap.* **787** (1972), p. 16.
38. L. J. Burdick and G. R. Mellman, *Bull. Seismol. Soc. Am.* **66**, 1485 (1976).

39. M. M. Clark, *U.S. Geol. Surv. Prof. Pap.* 787 (1972), p. 55.
40. J. E. Ebel and D. V. Helmberger, *Bull. Seismol. Soc. Am.* 72, 413 (1982).
41. T. H. Heaton and D. V. Helmberger, *ibid.* 67, 315 (1977).
42. T. C. Hanks and M. Wyss, *ibid.* 62, 561 (1972).
43. H. Kanamori and P. C. Jennings, *ibid.* 68, 471 (1978).
44. M. D. Petersen *et al.*, *Tectonics* 10, 1187 (1991).
45. W. Thatcher and R. M. Hamilton, *Geol. Soc. Am. Bull.* 63, 647 (1973).
46. A. L. Bent, D. V. Helmberger, R. J. Stead, P. Ho-Liu, *Bull. Seismol. Soc. Am.* 79, 500 (1989).
47. H. Magistrale, L. Jones, H. Kanamori, *ibid.* p. 239.
48. S. A. Sipkin, *ibid.* p. 493.
49. R. V. Sharp *et al.*, *ibid.*, p. 252.
50. I thank S. Boundy-Sanders for discussions about this material and for review of the manuscript and three reviewers for their helpful comments.

13 October 1992; accepted 9 February 1993

Detection of HIV-1 DNA and Messenger RNA in Individual Cells by PCR-Driven *In Situ* Hybridization and Flow Cytometry

Bruce K. Patterson, Michele Till, Patricia Otto, Charles Goolsby, Manohar R. Furtado, Lincoln J. McBride, Steven M. Wolinsky*

Human immunodeficiency virus type-1 (HIV-1) DNA and messenger RNA sequences in both cell lines and blood obtained directly from HIV-1-infected patients were amplified by polymerase chain reaction and hybridized to fluorescein-labeled probes *in situ*, and the individually labeled cells were analyzed by flow cytometry. After flow cytometric analysis, heterogeneous cell populations were reproducibly resolved into HIV-1-positive and -negative distributions. Fluorescence microscopy showed that the cellular morphology was preserved and intracellular localization of amplified product DNA was maintained. Retention of nonspecific probe was not observed. Analysis of proviral DNA and viral messenger RNA in cells in the blood of HIV-1-infected patients showed that the HIV-1 genome persists in a large reservoir of latently infected cells. With the use of this technique it is now possible to detect single-copy DNA or low-abundance messenger RNA rapidly and reproducibly in a minor subpopulation of cells in suspension at single-cell resolution and to sort those cells for further characterization.

Interactions between HIV-1 and its host cell extend across a wide spectrum, from latent to productive infection. The virus can persist in cells as unintegrated DNA (1), as integrated DNA with alternative states of viral gene expression (2), or as a defective DNA molecule (3). Determining the fraction of cells in the blood that are latently or productively infected is important for the understanding of viral pathogenesis and in the design and testing of effective therapeutic interventions. Determining the number of infected cells in a heterogeneous cell population and the proportion of those cells that are transcriptionally quiescent requires the unambiguous identification of low-abundance proviral DNA and viral mRNA at single-cell resolution (4, 5).

Detection of rare cells containing specific nucleic acid sequences has been confounded by the low copy number of the

target sequence, variation in sequence specificity, and the inability to isolate these cells from a heterogeneous population. Rare target sequences can be detected *in vitro* with quantitative polymerase chain reaction (PCR) (6, 7), but the product DNA signal is averaged for the number of input cells that are lysed; thereby the association with individual cells is lost. Although conventional *in situ* hybridization can unambiguously identify target sequences in a single cell, a low copy number target sequence may not be detected. The combination of PCR with *in situ* hybridization allows the target sequence to be amplified above the limit of detection while maintaining the cellular architecture (4, 5), but a large number of microscopic fields need to be surveyed by a trained observer to demonstrate a rare affected cell.

Flow cytometric detection of DNA sequences in nuclei has been attained by means of fluorescein-linked DNA probes complementary to total genomic DNA (8) or highly repetitive chromosome-specific sequences (9). Flow cytometry has also been used to detect fluorescein-labeled probes hybridized *in situ* to high-abundance α -actin mRNA (10) or ribosomal RNA (11) in populations of cells. The *bcr-abl* fusion gene

has been detected in the human K562 myeloid leukemia cell line by flow cytometry after *in situ* nested-PCR amplification using fluorescein-labeled primers (12). Unfortunately, multiple amplification reactions, poor retention of product DNA within the cell, and the potential for mispriming by this technique frequently compromise both sensitivity and specificity. Detection of rare nucleic acid sequences in a minor subpopulation of cells in suspension by flow cytometry has not been demonstrated.

To detect single-copy proviral DNA or low-abundance viral mRNA in a subpopulation of cells in suspension, we used PCR-driven *in situ* hybridization with fluorescein-linked oligonucleotide probes and flow cytometry. Intracellular DNA and RNA sequences were preserved *in situ* with a nonaldehyde, noncross-linking, water-soluble fixative [Streck Tissue Fixative (STF); Streck Labs, Omaha, Nebraska], and the cell membrane was permeabilized with proteinase K (1 μ g/ml). Specific intracellular nucleic acid sequences were amplified by a PCR protocol in which bulky digoxigenin-linked deoxyuridine 5'-triphosphate (dUTP) was used to produce a product DNA that remained in place *in situ*. Product DNA was then hybridized *in situ* with an internally conserved, fluorescein-labeled oligonucleotide probe, and the cell suspension was analyzed by flow cytometry.

To demonstrate PCR-driven *in situ* amplification of viral sequences in cells in suspension, we amplified proviral DNA sequences in HIV-1-infected 8E5/LAV cells (13), which contain a single copy of proviral DNA, by PCR with HIV-1-specific primers and digoxigenin-linked dUTP (14). The cell suspension containing known ratios of 8E5/LAV cells and uninfected peripheral blood mononuclear cells (PBMCs) was centrifuged onto microscope slides that had been treated with Denhardt's solution. Cells were visualized by light microscopy after immunohistochemical staining (15) with alkaline phosphatase-conjugated anti-digoxigenin (Fig. 1A). A 100% sensitivity and a 98% specificity was attained on the basis of duplicate 500-cell counts. Each experiment was done in triplicate. Nonspecific alkaline phosphatase-conjugated anti-digoxigenin staining was not detected.

The procedure was optimized for hybridization of fluorescein-labeled oligonucleotide probes to cells in suspension under conditions of high stringency (10). Oligonucleotides with fluorescein-linked nucleotides positioned at 10- to 12-nucleotide intervals were synthesized by phosphoramidite chemistry (16). Intracellular product DNA was hybridized to either the specific viral probe or a noncomplementary probe *in situ* (17). Intracellular HLA-DQ α product DNA sequences hybridized to either complementary

B. K. Patterson and C. Goolsby, Department of Pathology, Northwestern University Medical School, Chicago, IL 60611.

M. Till, P. Otto, M. R. Furtado, S. M. Wolinsky, Department of Medicine, Northwestern University Medical School, Chicago, IL 60611.

L. J. McBride, Department of DNA Analysis, Applied Biosystems Inc., Foster City, CA 94404.

*To whom correspondence should be addressed.